PROCEEDINGS OF SPIE

SPIEDigitalLibrary.org/conference-proceedings-of-spie

Investigating probabilistic constellation shaping for dual-polarization PAM8 signals at different data rates

Kayden LC Kaller, Mihail Raytchev, Ahmed Galib Reza, Marcos Troncoso Costas, Liam Barry, et al.

Kayden LC Kaller, Mihail Raytchev, Ahmed Galib Reza, Marcos Troncoso Costas, Liam Barry, Ahmad Atieh, "Investigating probabilistic constellation shaping for dual-polarization PAM8 signals at different data rates," Proc. SPIE 12429, Next-Generation Optical Communication: Components, Sub-Systems, and Systems XII, 124291E (15 March 2023); doi: 10.1117/12.2648047

SPIE.

Event: SPIE OPTO, 2023, San Francisco, California, United States

Investigating probabilistic constellation shaping for dual-polarization PAM8 signals at different data rates

Kayden LC Kaller[a], Mihail Raytchev[a], Ahmed Galib Reza[b], Marcos Troncoso Costas[b], Liam Barry[b], Ahmad Atieh*[a],
[a]Optiwave Systems Inc, Ottawa, Ontario, K2E 8A7, Canada; [b]School of Electronic Engineering, Dublin City University, Glasnevin, Dublin 9, Ireland

ABSTRACT

DP-PAM8 modulated signals with probabilistic constellation shaping (PCS) are investigated for ultrahigh-data rates with diverse shaping strengths and DGD values using direct detection for short distances mainly seen in data centers. The investigation is conducted using numerical simulation, where system performance improvement is achieved when PCS is used. The probabilistic shaping mitigated the uncompensated DGD and dispersion effects in the transmission system. We found that the high-powered symbols close the eye causing high symbol error. Applying PCS opens the eye of the high-powered symbols but closes the eye for low-powered ones. Thus, optimization of the strength of shaping is necessary to get the best performance. Experiments were conducted to investigate the effect of probabilistic shaping on PAM8 system amplified using an optical semiconductor amplifier (SOA). A single polarization PAM8 case was only demonstrated due to accessibility limitations of required parts for dual-polarization PAM8.

Keywords: DP-PAM8, probabilistic constellation shaping, probabilistic shaping strength, differential group delay (DGD)

1. INTRODUCTION

The demand for higher data rates is ever increasing to meet the pressure of exploding information transmission needs for the different services in the market. These services include social networking, videoconferencing, multimedia streaming, etc. Tackling the increasing of the transmission data rates is achieved using dense wavelength division multiplexing (DWDM), spatial multiplexing through using single-core multimode fiber (SMF), multicore single mode fiber, multicore multimode fiber, and finally using advanced modulation schemes where symbols; created from more than one bit, are transmitted in a single time slot such as quadrature amplitude modulation (QAM) and pulse amplitude modulation (PAM) schemes [1-4]. Probabilistic constellation shaping (PCS) is a modern technique that offers increasing systems tolerance to noise and fiber nonlinearity through reducing launched average power. One type of PCS is probabilistic amplitude shaping (PAS) technique that can be applied to higher modulation schemes such as PAM and QAM, by decreasing the entropy of the base format. This is achieved by altering the distribution of the symbols in a transmitted sequence, such that the low-powered symbols occur at a higher rate of occurrence. Due to this emphasis on low-powered symbols, PAS can be applied in long-haul QAM systems for the inherent decrease in nonlinear effects of the optical fiber, which allows for increased reach [5,6]. State of the art PAS systems incorporate dual-polarized (DP) QAM formats for further increased system capacity [7]. However, to the best of our knowledge, no information regarding DP-PAM systems with PAS exist in the literature. Research has been conducted into PAS-PAM systems, and DP-PAM systems, but none combining the two techniques [8,9].

In this paper, we proposed using DP-PAS-PAM8 systems for datacenters where ultrahigh system capacities are desired. We used numerical simulations to assess the system performance for different data rates, differential group delays (DGD) and shaping rates for direct detection cases. No polarization compensation or DSP processing were used for direct detection cases. The performance was compared to cases without probabilistic shaping. It was found that without shaping, the high-powered symbols close the eye causing high symbol errors, which was due to no compensation of DGD and dispersion at the highest PAM8 levels. However, applying PAS open the eye of the high-powered symbols, but close the eye for low-powered ones. Thus, optimization of the shaping rate is needed to get the best performance, where the PAS scheme was used to diminish the detrimental effects in the direct-detection DP-PAM systems.

*ahmad.atieh@optiwave.com; phone 1 613 224-4700; fax 1 613 224-4706; optiwave.com

Next-Generation Optical Communication: Components, Sub-Systems, and Systems XII, edited by Guifang Li, Kazuhide Nakajima, Atul K. Srivastava, Proc. of SPIE Vol. 12429, 124291E

· 0277-786X · doi: 10.1117/12.2648047

2. NUMERICAL SIMULATION

PAM systems can be readily adapted to apply the PAS technique, where the coding/decoding components are replaced by constant composition distribution matcher (CCDM) coders. The CCDM coder at the transmitter end maps an input binary sequence to an output *M*-ary symbol sequence containing the desired symbol distribution. At the receiver end, the CCDM decoder gets the desired bit stream after the decision circuit. Direct detection (DD) and coherent detection (CD) are investigated for the different transmission cases for PAM4 and PAM8 systems. Digital signal processors (DSP) with multifunctionality are used only in the CD cases. Different algorithms are used in the DSP such as probability-aware algorithms, low pass filter, adaptive equalization, frequency offset estimation, carrier phase estimation, and timing recovery. The state of polarization (SOP) of the transmitted modulated signals is compensated independently of the DSP component.

Fig. 1 illustrates the block diagram of the investigated coherent and direct detection DP-PAS-PAM4/8 systems. Coherent detection was used for DP-PAM4 systems, while direct detection was used for DP-PAM8 systems. The performance of the system is investigated using commercial OptiSystem software. Numerical simulations were conducted at different rates, 400Gbps, 200Gbps, 100Gbps and 50Gbps for different shaping strengths under diverse DGD values. A Bit Error Rate Test (BERT) Set generates a pseudorandom bit sequence that is split using a serial to parallel converter, and fed into two PAM/PAS Sequence Generators that use constant composition distribution matching to encode the binary sequences into *M*-ary sequences, with symbol occurrences determined through the Maxwell-Boltzmann distribution. For PAM4 simulations, 4 frames of codewords containing 1,024 symbols were used, while the PAM8 systems frame has codewords of 8,192 symbols. The overall bit sequence length was adjusted depending on the simulated entropy. The M-ary Pulse Generator components generate the electrical signals that are modulated using Mach-Zehnder Modulators to create the respective X and Y polarization signals. A polarization splitter is used to split a 10 dBm, 1550 nm Continuous Wave (CW) laser to carry the modulated signal at each polarization state.

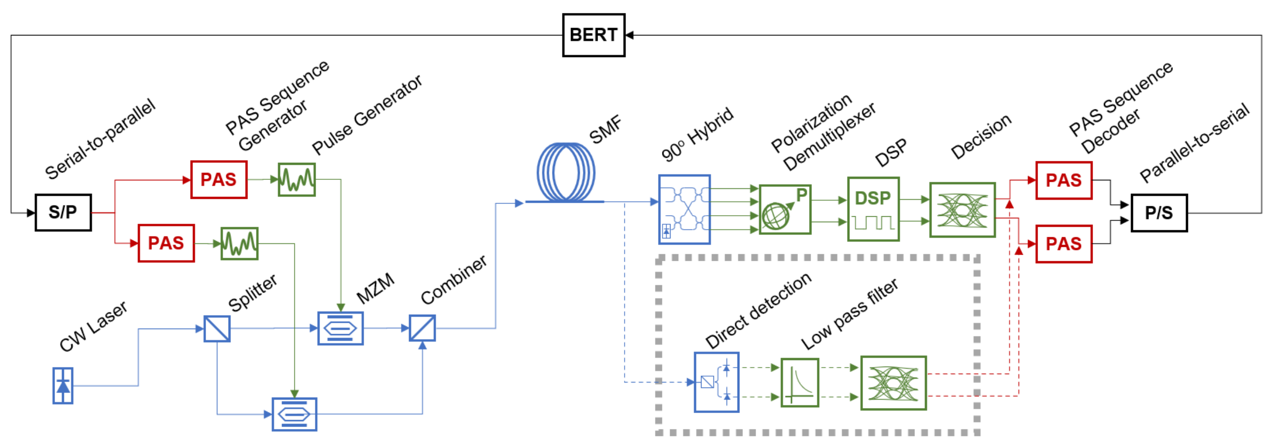

Figure 1. DP-PAS-PAM4/8 system block diagram. The dotted box is used for the direct detection case.

The modulated signals are combined using a polarization combiner and transmitted through standard telecommunication single mode optical fiber. For coherent detection, the received signal is detected using an optical coherent receiver. A format-independent polarization demultiplexing algorithm for intensity modulated signals is used to recover the original transmitted polarization states [5]. The received X and Y electrical signals were processed using a Digital Signal Processor (DSP) component followed by a Decision component and PAS decoder. The number of symbol errors (SE) and the error vector magnitude (EVM) are calculated in the Decision component. The adaptive equalization in the DSP of the system can be automatically or manually optimized. The range of the radius detected (RD) parameters was properly set in the auto-mode to achieve better results in terms of EVM and SE by locating the global minima. For direct detection cases, no polarization compensation or DSP processing were used, aside from a low pass filter.

3. RESULTS AND DISCUSSIONS

Fig. 2 shows the investigated data rates versus the maximum possible achieved ranges with zero symbol errors at no shaping (entropy of 2) and DGD of 0.2 ps/km for DP-PAM4. These ranges are used to further investigate the performance of the DP-PAS-PAM4/8 systems for different DGD values and strengths of amplitude shaping. Fig. 3 and Fig. 4 illustrate the calculated number of SE and EVM for 200Gbps DP-PAS-PAM4 signal propagated through different SMF lengths with a DGD value of 0.2 ps/km. Similar simulations were done at the date rate of 400Gbps, 100Gbps and 50Gbps. These two figures show that the best performance for DP-PAS-PAM4 is achieved for no shaping or very weak shaping with entropy close to 2. It is also important to discuss the effect of using SOP compensation under different DGD values as shown in Fig. 5 at an entropy of 1.973 for 100Gbps PAM4 modulated signal. It is clear that compensating the SOP causes almost no fluctuations in the symbol errors.

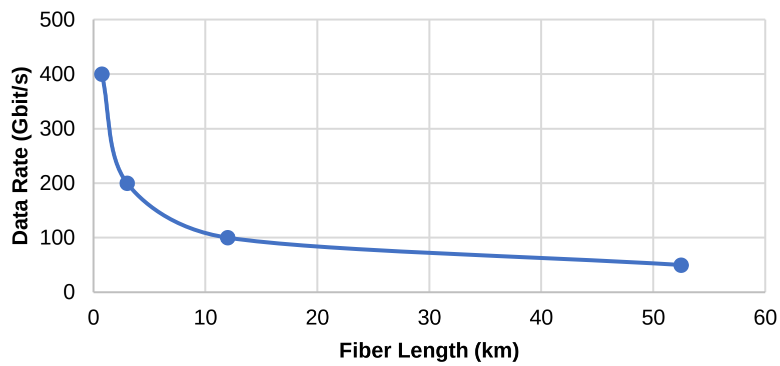

Figure 2. Investigated data rates versus maximum possible achieved range for DP-PAM4.

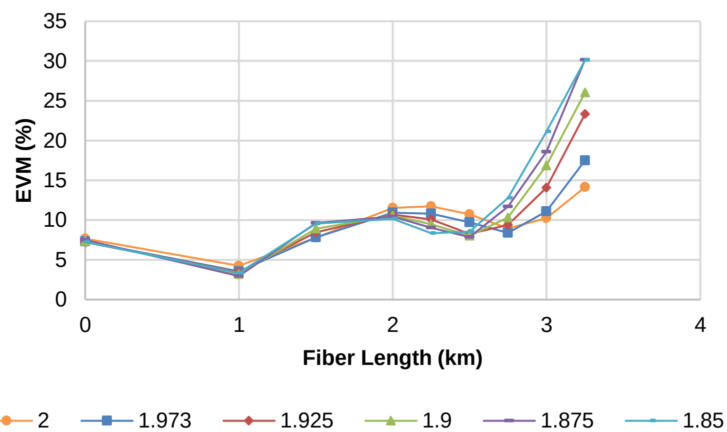

Figure 3. EVM of 200Gbps DP-PAS-PAM4 signal transmitted over various lengths of SMF at 0.2 ps/km DGD.

Fig. 6 displays the calculated number of symbol errors for a 400G DP-PAS-PAM8 transmitted signal with direct detection under different SMF lengths with a DGD value of 0.2 ps/km. The unshaped signal displays a significant number of errors between 0.4-1 km. Applied PAS mitigates errors within this region and can be optimized at a specified length of fiber to produce error-free transmission. Fig. 7 shows the calculated SE for 0.6 km of fiber at different shaping rates, while Fig. 8 shows the electrical eye diagrams with and without shaping. It can be seen from Fig. 8 that without shaping, the high-powered symbols have closed the eye causing high SE. Applying PAS opens-up the eye of the high-powered symbols but closes the eye for low-powered ones. Thus, optimization is done in Fig. 7. We found that the eye closure in the 0.4-1 km region is due to uncompensated of DGD and dispersion at highest PAM8 level. This suggests that PAS can be used to diminish polarization drift in the direct-detection DP-PAM systems.

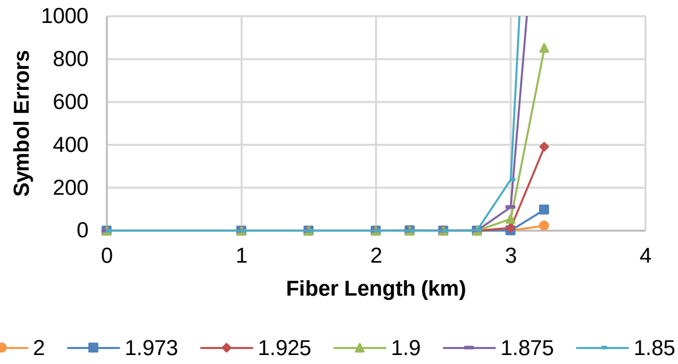

Figure 4. Measured SE of 200Gbps DP-PAS-PAM4 signal transmitted over various lengths of SMF at 0.2 ps/km DGD.

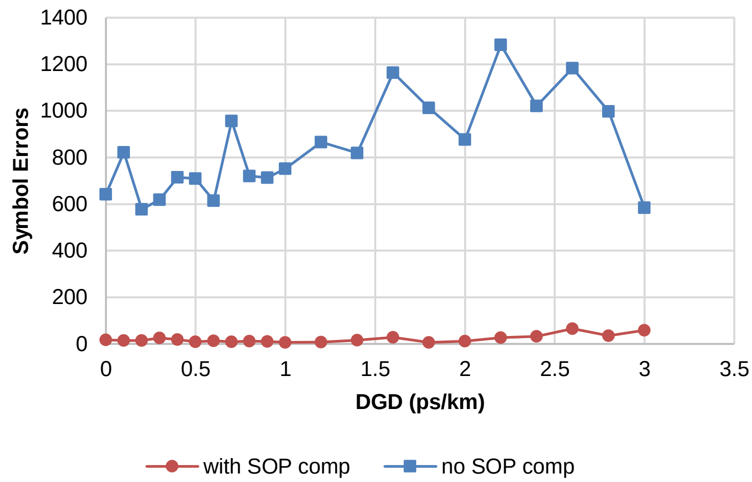

Figure 5. Measured SE for 100Gbps DP-PAS-PAM4 signal transmitted over 13km of SMF under different DGD effect.

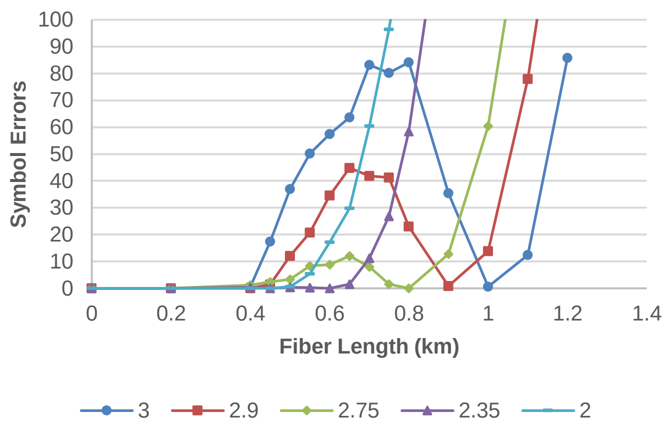

Figure 6. Measured SE of 400Gbps DP-PAS-PAM8 signal transmitted over various lengths of SMF at 0.2 ps/km DGD.

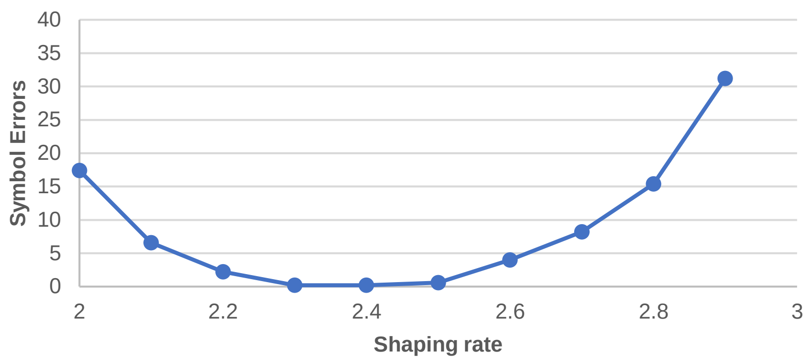

Figure 7. Symbol error for different applied PAS for a 400Gbps DP-PAS-PAM8 signal transmitted at 0.6 km.

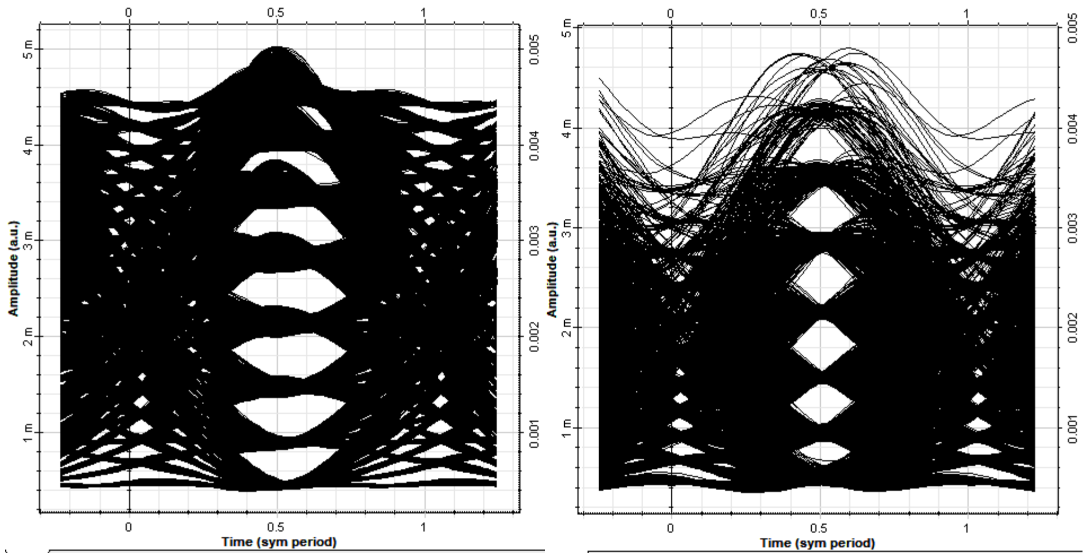

Figure 8. Eye diagrams of a 400Gbps DP-PAS-PAM8 signal at 0.6 km without (left) and with (right) applied shaping.

4. EXPERMENTAL SETUP

Fig. 9 shows the experimental setup used to characterize the effect of probabilistic pulse shaping on PAM8 modulated signal. A PS-PAM8 signal is generated and transmitted over 1km of SMF-28 fiber after amplifying using SOA. The 50-Gbaud PS-PAM8 symbols with the sequence length of 216 are digitally up-sampled by 1.75 times to match the base clock frequency of the arbitrary waveform generator (AWG) followed by root-raised cosine (RRC) filtering with a roll-off factor of 0.1, and digital pre-distortion to obtain equidistant PAM-8 levels after modulation. The PS-PAM8 signals are then sent to a 32GHz AWG (Keysight M8196A) running at 87.5GSa/s. The AWG output of Vpp = 180mV is sent to a 23dB gain RF amplifier with 55GHz bandwidth, which drives an over 20-GHz single-ended Mach-Zehnder modulator (MZM) that is biased at quadrature and modulates an external cavity laser (ECL) with the optical frequency of 193.25 THz. To emulate a hyper-scale DCI scenario, we reduce the output power of the MZM to -8dBm with a variable optical attenuator (VOA) before sending it to an SOA, which produces an optical output power of 7dBm that is directly launched into a 1km SMF. After fiber transmission, a VOA is used at the receiver side to adjust the received optical power (ROP) before directly detecting by a 70GHz photodetector (PD) for optical-to-electrical conversion. The output of the PD is amplified by a 23dB gain RF amplifier with 55GHz bandwidth. Lastly, the signal is captured with a real-time scope operating at 100GSa/s. For signal recovery, by using a receiver-side offline DSP block, the captured signal is resampled at one sample/symbol followed by matched filtering, symbol synchronization, and linear equalization using a 26tap FFE to mitigate the distortions in the signal. The system performance is compared with a non-shaped PAM8 modulated signal for different input power levels the SOA as shown in Fig. 10. Numerical simulation was conducted on a setup that replicates the experimental system with no FEC applied to the transmitted data. The symbol rate versus received power level is shown in Fig. 11. Numerical simulations of the experiment using OptiSystem software showed similar performance improvement for PS case as illustrated in Fig. 12 for the calculated symbol error rate (SER). The attenuator controls the power level of the PMA8 signal applied to the SOA.

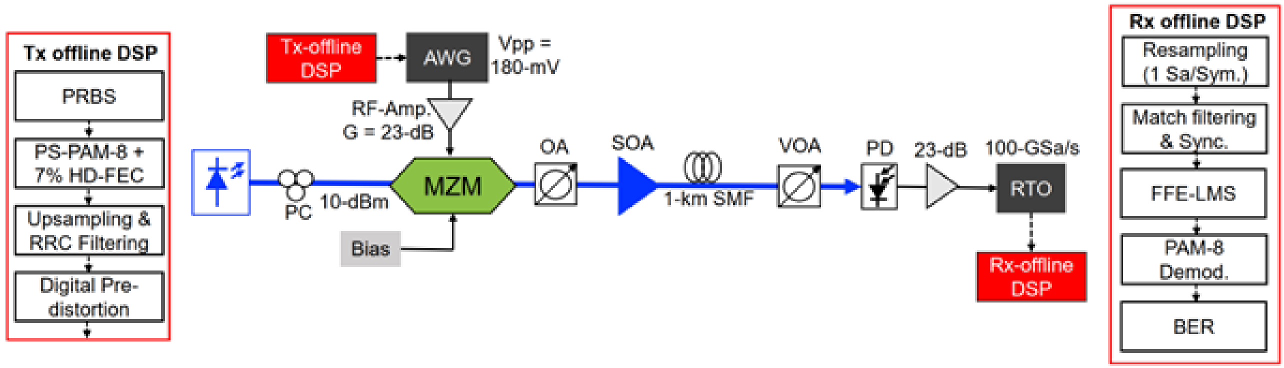

Figure 9. Experimental setup used for PAM8-PAS transmission system.

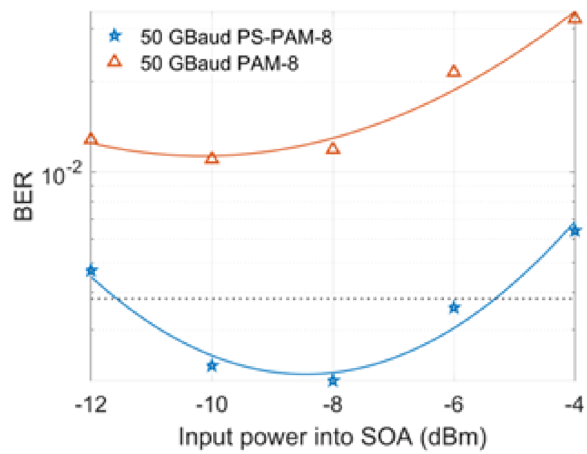

Figure 10. BER vs. input power into the SOA for 50 GBaud PAM8 and PS-PAM8 transmission when receiver optical power is 0 dBm.

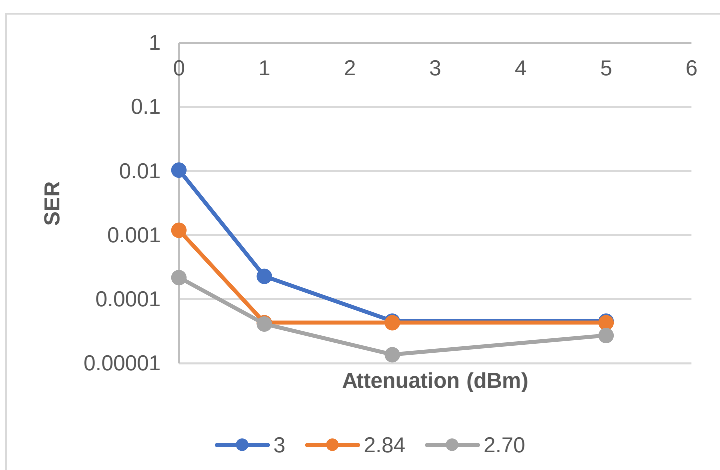

Figure 11. SER vs. input power into the SOA controlled by the attenuator setting.

5. CONCLUSIONS

Dual-polarized PAM4/8 modulated signals with probabilistic amplitude shaping were investigated for direct detection and coherent detection. Different data rates are transmitted over single mode optical fiber with diverse DGD. Numerical simulations of 400Gbps, 200Gbps, 100Gbps and50Gbps under different shaping strengths are considered in this work. Coherent detection systems displayed no benefit to the use of PAS for both PAM4 and PAM8. However, direct-detection systems showed significant improvement with PAS, where shaping was used to mitigate uncompensated polarization drift effects from the DP-PAS-PAM8 transmitted systems. Users are recommended to apply probabilistic shaping to dual-polarization PAM8 transmission systems and use proper shaping rate to get the best performance. Experimental demonstration of single opalization PS-PAM8 signal showed that probabilistic pulse shaping improves system performance.

REFERENCES

[1] Zhu, B. Taunay, T. F Yan, M. F. Fishteyn, M. Oulundsen, G. and Vaidya, D. "70-Gb/s Multicore Multimode Fiber Transmission for Optical Data Links," *IEEE Photonics Technology Letters*, 22(22), (2010). DOI: 10.1109/LPT.2010.2070490

[2] Murshid, S. H. and Chakravarty, A. "Attenuation and Bit Error rate for Four Copropagating Spatially Multiplexed Optical Communication Channels of Exactly Same Wavelength in Step Index Multimode Fibers," in *Enabling Photonics Technologies for Defense, Security, and Aerospace Applications*, Orlando, United States, 80540P (2011). DOI: 10.1117/12.884408

[3] Sakamoto, T. Saitoh, K. Saitoh, S. Shibahara, K. Wada, M. Abe, Y. Urushibara, A. Takenaga, K. Mizuno, T. Matsui, T. Aikawa, K. Miyamoto, Y. and Nakajima, K. "Six-Mode Seven-Core Fiber for Repeated Dense Space-Division Multiplexing Transmission," *Journal of Lightwave Technology*, 36(5), (2018). DOI: 10.1109/JLT.2018.2797361

[4] Sadot, D. Dorman, G. Gorshtein, A. Sonkin, E. and Vidal, O. "Single channel 112Gbit/sec PAM4 at 56Gbaud with digital signal processing for data centers applications," *Optics Express*, 23(2), (2015). DOI: 10.1364/OE.23.000991

[5] Dúill, S. P. Ó. and Barry, L.P. "Format-independent polarization-demultiplexing technique for dual-polarization intensity modulated signals," *Applied Optics*, 55(7), (2016). DOI: 10.1364/AO.55.001658

[6] Buchali, F. Steiner, F. Böcherer, G. Schmalen, L. Schulte, P. and Idler, W. "Rate adaptation and reach increase by probabilistically shaped 64-QAM: An experimental demonstration," *Journal of Lightwave Technology*, 34(7), (2016). DOI: 10.1109/JLT.2015.2510034

[7] Chen, Y. W. Kuzmin, K. Zhang, R. Poirier, M. Tomimoto, T. Zarris, G. Moore, R. Chen, C. Wu, W. Huang, J. and Boudreau, M. "InP CDM and ICR Enabled 128Gbaud/ DP-16QAM-PS and 120Gbaud/DP-QPSK Long-Haul Transmission," in *IEEE Photonics Technology Letters*, 34 (9), (2022). DOI: 10.1109/LPT.2022.3165484

[8] Wiegart, T. Da Ros, F. Yankov, M. P. Steiner, F. Gaiarin, S. and Wesel, R. D. "Probabilistically shaped 4-PAM for short-reach IM/DD links with a peak power constraint," *Journal of Lightwave Technology*, 39(2), (2021). DOI: 10.1109/JLT.2020.3029371

[9] El-Fiky, E. Osman, M. Sowailem, M. Samani, A. Patel, D. Li, R. Saber, M. G. Wang, Y. Abadia, N. D'Mello, Y. and Plant, D. V. "200 Gb/s transmission using a dual-polarization O-Band silicon photonic intensity modulator for Stokes vector direct detection applications," *Optics Express*, 25 (24), (2017). DOI: 10.1364/OE.25.030336.